GENERIC MAPS OF THE PROJECTIVE PLANE WITH A SINGLE TRIPLE POINT

GREG HOWARD*
FEDERAL RESERVE BOARD OF GOVERNORS AND
UNIVERSITY OF NORTH CAROLINA, CHAPEL HILL
SUE GOODMAN
UNIVERSITY OF NORTH CAROLINA, CHAPEL HILL

Abstract. Cromwell and Marar [CM] present an analysis of semi-regular (generic) surfaces with a single triple-point and connected self-intersection set. Six of their surfaces are the projective plane, including Boy's surface and Steiner's surface. We build on their work by incorporating twists similar to that of Apery's immersion of the projective plane and show that with a few additional surfaces, all such generic maps of the projective plane are now identified.

In *Models of the Real Projective Plane*, Apery [A] describes an immersion of the projective plane into $\mathbb{R}^3$ with a single triple point but with image homeomorphically distinct from Boy's surface. This immersion does not seem to be well known but is explored in greater detail in [GK]. An essential difference between the two immersions is that there is a twist in a neighborhood of one loop of the self-intersection set. Following [GK], we denote Boy's surface as $\mathcal{B}$ and the alternative immersed surface as $\mathcal{G}$. As shown in [GK], up to ambient isotopy these, and their mirrors, are the only immersions of the projective plane with connected self-intersection set and a single triple point.

Cromwell and Marar [CM] present an analysis of semi-regular (generic) surfaces with a single triple-point and a connected self-intersection set. Six of the surfaces they present are the projective plane, including Boy's surface and Steiner's surface. In this paper, we build on their work by adding twists similar to that of Apery's immersion and showing that with a small number of additional surfaces, all possibilities for the projective plane (up to homeomorphism) are now identified. Note that, unlike Cromwell and Marar, we restrict to the projective plane to keep the number of possibilities relatively small.

1991 *Mathematics Subject Classification.* 57R45,57R42.
Key words and phrases. generic maps, projective plane, triple point.

*The views of this paper are solely the responsibility of the authors and should not be interpreted as reflecting the views of the Board of Governors of the Federal Reserve System or of any other person associated with the Federal Reserve System.

In Section 1, we provide preliminary definitions and results. In Section 2, we present the new examples and proof that the list is complete. Section 3 illustrates homotopy relationships between these surfaces.

The authors would like to thank Alex Mellnik for his computer graphics and help; Jane Hawkins and Justin Sawon for their constructive comments and service on the thesis panel; and Richard Rimanyi, Scott Carter, and Washington Marar for their helpful feedback. We are grateful for monetary support of the Honors Department at UNC.

Section 1: Preliminaries

Let M be a closed surface and $f : M \to \mathbb{R}^3$ be a smooth map. Recall that a Whitney umbrella, or *pinch point*, is a singularity which locally, for some choice of coordinates, is given by $f(u,v) = (uv, u, v^2)$. Whitney [W] proved that any map can be approximated by one with singularities only of this type. Hence we call f *generic* if it is an immersion except for a finite number of pinch points. The image is what we will refer to as a *generic surface* (semi-regular surface in [CM]).

We will restrict our classification to the case where M is the projective plane $\mathcal{P}$. We can represent generic maps on the standard plane model of $\mathcal{P}$ by indicating the self-intersection set and any pinch points. Each double point arc is on the plane model twice to represent the two places it occurs. For example, the cross-cap model of $\mathcal{P}$ has two pinch points connected by an orientation-reversing double point arc. So we represent it as in Figure 1a. The two dots represent pinch points and the arcs joining them represent the double-point set. The three pre-image points of a triple point are represented by intersections of double point arcs. For example, Figure 1b represents Boy's surface $\mathcal{B}$.

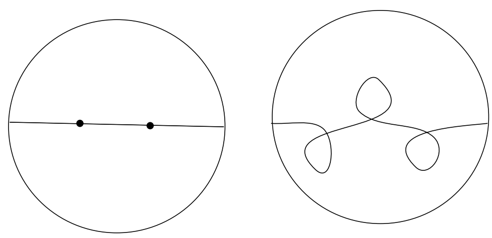

Figure 1

Another way of visualizing a generic surface is the neighborhood of the self-intersection set. Let $\mathcal{S}$ denote the self-intersection set of the image $f(\mathcal{P})$, and $N(\mathcal{S})$ a small neighborhood of $\mathcal{S}$ in $f(\mathcal{P})$. This is referred to as a *partial surface* in [CM]. As illustration, we show in Figure 2 for $\mathcal{B}$ and $\mathcal{G}$.

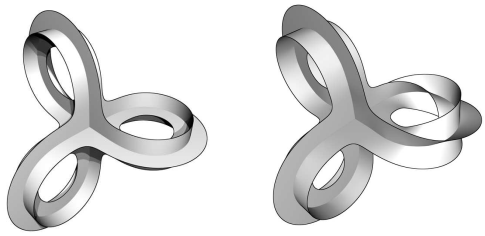

Figure 2

The proof in [S] that no embedding of the projective plane exists in $\mathbb{R}^3$ can be readily generalized to show that generic surfaces in $\mathbb{R}^3$ are two-sided; that is, a positive and negative side to the surface can be consistently designated.

Proposition 1.1. *All closed generic surfaces in $\mathbb{R}^3$ are two-sided.*

Proof. Let $f(M)$ be a closed generic surface in $\mathbb{R}^3$. Suppose it is not two-sided. Then, there exists an orientation reversing loop λ somewhere along the surface. Starting at any point on λ, choose a short normal vector of length δ. Push λ off $f(M)$ to create a curve λ' that is δ away from λ and not meeting $f(M)$. Then connect the curve you just drew through the point. This curve λ' now becomes a loop that intersects the surface exactly once.

Furthermore, since the image is in $\mathbb{R}^3$, the loop bounds an embedded surface K that is transversal to the image $f(M)$ and missing the pinch points. Let $g : K \to \mathbb{R}^3$ be the map from the surface with boundary into $\mathbb{R}^3$. As Samuelson argues, by transversality, it consists of closed curves in the interior of K plus arcs that terminate on the boundary. If they do terminate, they must terminate in two places. Therefore, the number of points on the boundary must be even. But by construction, the number of points on the boundary of $g^{-1}(f(M))$ is one, yielding a contradiction. □

Arguments in the remaining sections will make use of a few other results, including the Izumiya-Marar formula and a generalization of Banchoff's theorem on the parity of triple points to the setting of generic maps. Although the latter can be shown from Szucs [Sz] and is also a special case of a result on Nuño Ballesteros and Saeki [NS], we include an alternative proof here (Proposition 1.3) since it is quite simple and gives a somewhat different proof to the classical result of Banchoff (more in the spirit of [FT]).

Proposition 1.2. *(Izumiya-Marar [IM]) The Euler characteristics of a surface M and any generic image of M, $f(M)$, are related by the number of triple points and pinch points in the generic surface, by the following relationship:*

$$\chi(f(M)) = \chi(M) + \#(\text{triple points}) + \frac{\#(\text{pinch points})}{2}$$

For the next result, we consider an ε-displacement of a generic surface: a collection of embedded orientable surfaces obtained by pushing off the generic surface to one side. That is, designate one side of $f(M)$ as positive. For a sufficiently small ε, take an ε-neighborhood of $f(M)$ in $\mathbb{R}^3$. Let $L\varepsilon$ be the boundary of the ε-neighborhood on the positive side. For example, for a cross-cap surface, $L\varepsilon$ would be a sphere, regardless of which side one pushes to. In general, the choice of sides can give different $L\varepsilon$. In particular, in the neighborhood of a pinch point, pushing to one side locally gives two sheets, while pushing to the other side gives one. See Figure 3. We say a pinch point is *double sheeted* if locally $L\varepsilon$ has two components, and *single sheeted* if only one. Note that this clearly depends on the choice of what we call the positive side.

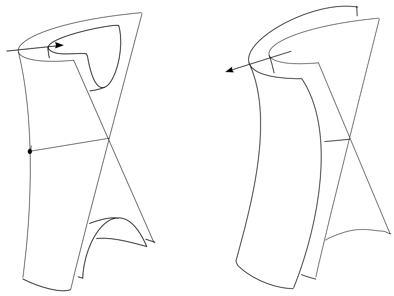

Figure 3

Proposition 1.3. *Let $f(M)$ be a generic surface in $\mathbb{R}^3$ with a designated positive side. Then,* $\chi(M) + \#(\text{triple points}) + \#(\textit{double-sided pinch points}) \equiv 0 (\bmod 2)$.

Proof. Begin with a cell decomposition of $f(M)$ with vertices at pinch points and triple points and edges along arcs of double points. Take a corresponding cell decomposition for $L\varepsilon$ (so that k-cells of $L\varepsilon$ project to k-cells of $f(M)$). We consider the local differences in Euler characteristic between $L\varepsilon$ and $f(M)$. At a double-sheeted pinch, the pinch point on $f(M)$ corresponds to two different vertices on $L\varepsilon$, adding one to the Euler characteristic. A single-sheeted pinch point corresponds to only one vertex on $L\varepsilon$. An arc of double points displaces to two edges on $L\varepsilon$, subtracting one from the Euler characteristic. A triple point on $f(M)$corresponds to four vertices on $L\varepsilon$,, and the Euler characteristic increases by 3.

Let $e_{f(M)}$ represent the number of edges of $f(M)$. The above three facts give that

$$\chi(f(M)) = \chi(L\varepsilon) + e_{f(M)} - 3 \cdot \#(\text{triple points}) - \#(\text{double-sided pinch points})$$

where $\chi(L\varepsilon)$ is simply the sum of all the Euler characteristics of all the embedded surfaces making up $L\varepsilon$.

Each triple point has six edges emanating out of it. Each pinch-point has a single edge emanating out of it. Each edge ends in two places. Therefore a standard Riemann- Hurwitz argument gives that the total number of edges in the self-intersection set is

$$e_{f(M)} = \frac{1}{2}[6 \cdot \#(\text{triple points}) + \#(\text{pinch points})].$$

Noting that the number of pinch points is the sum of the number of single-sided plus double-sided pinches gives us

$$\chi(f(M)) = \chi(L\varepsilon) + \frac{1}{2}\cdot\#(\text{single-sided pinch points}) - \frac{1}{2}\cdot\#(\text{double-sided pinch points}).$$

By the Izumiya-Marar formula,

$$\chi(f(M)) = \xi(M) + \#(\text{triple points}) + \frac{1}{2}\cdot\#(\text{pinch points}),$$

so

$$\chi(L\varepsilon) - \#(\text{double-sided pinch points}) - \#(\text{triple points}) = \chi(M).$$

However we know $\chi(L\varepsilon)$ is even because it is the sum of the Euler characteristics of orientable surfaces. So $\chi(M) + \#(\text{triple points}) + \#(\text{double-sided pinch points})$ is even. □

Note that switching the orientation switches each double-sheeted pinch point to a single-sheeted pinch point and vice versa. It is useful to re-formulate the above result so that it is independent of which side of $f(M)$ one chooses as positive. Define an *oppositely-oriented* pinch pair to be one with one single-sheeted and one double-sheeted pinch point. Note that any non-oppositely oriented pinch pair will have zero or two double-sided-pinches, so the parity of double-sided pinch points is the same as oppositely-oriented pinch pairs.

Corollary 1.4. *For any generic surface,*

$$\chi(M) + \#(\text{triple points}) + \#(\text{oppositely-oriented pinch pairs}) \equiv 0 (\text{mod}\, 2).$$

Banchoff's classical result on immersed surfaces follows immediately by setting the number of pinch points equal to zero.

Corollary 1.5. *(Banchoff) An immersion of the projective plane must have at least one triple point.*

Lastly we note that there is a restriction on the number of boundary circles in $N(S)$ when we focus on generic maps of the projective plane.

Proposition 1.6. *The number of boundary edges of a neighborhood of the self-intersection set for a generic map of the projective plane is at least 4. If these edges all bound embedded disks in $f(\mathcal{P})$ then the number is exactly 4.*

Proof. By the Izumiya-Marar formula, we know that

$$\chi(f(\mathcal{P})) = \chi(\mathcal{P}) + \#(\text{triple points}) + \frac{1}{2}\cdot\#(\text{pinch points}) = 2 + \frac{1}{2}\cdot\#(\text{pinch points}).$$

On the other hand, one can calculate $\chi(\mathcal{P})$ directly. Once again construct a cell decomposition of $f(\mathcal{P})$ with vertices at pinch points and triple points and edges along arcs of double points. Any face of $\mathcal{P}$ must be planar; that is, a disk with holes. Let f_k be the number of faces with k boundary edges. We can add $(k-1)$ edges connecting existing vertices to create a cell decomposition of $\mathcal{P}$. Then we have

$$\begin{aligned}
v &= \#(\text{triple points}) + \#(\text{pinch points}) = 1 + \#(\text{pinch points}) \\
e &= \tfrac{1}{2} \cdot [6 \cdot \#(\text{triple points}) + \#(\text{pinch points})] + f_2 + 2f_3 + \cdots + (k-1)f_k \\
&= 3 + \tfrac{1}{2} \cdot \#(\text{pinch points}) + f_2 + 2f_3 + \cdots + (k-1)f_k \\
f &= f_1 + f_2 + \cdots + f_k.
\end{aligned}$$

Then

$$2 + \frac{1}{2} \cdot \#(\text{pinch points}) = \chi(f(\mathcal{P})) = -2 + \frac{1}{2} \cdot \#(\text{pinch points}) + f_1 - f_3 - 2f_4 \cdots - (k-2)f_k.$$

So $f_1 \geq 4$, giving that there are at least 4 boundary edges in $N(\mathcal{S})$. □

We end this section by summarizing several criteria that $N(\mathcal{S})$ must satisfy in order to be able to be completed to the image of a generic map of the projective plane.

i. The number of boundary components must be at least 4 (by Proposition 1.6).
ii. The number of oppositely-oriented pinch pairs must be even (by Corollary 1.4).
iii. Any boundary component of N(S) bounding a disk face must be unknotted and unlinked with any other boundary component and with the self-intersection set.
iv. If two double-point arcs emanating from the triple point are opposite each other (as positive and negative axes) are joined, then the number of quarter twists must be odd. If the two arcs are adjacent, then the number of quarter-twists must be even. This follows from Proposition 1.1 above and Lemma 3.1 of GK.

Section 2

Cromwell and Marar present six generic maps of the projective plane: 0_{A}, 2_{C}, 4_{A}, 4_{D}, 4_{F}, and 6_{A}. The numbers correspond to the number of pinch points they have, with 0_{A} being Boy's surface and 6_{A} being Steiner's. (Note that the lettering is not sequential because Cromwell and Marar consider surfaces besides the projective plane.)

With a single triple point and a connected self-intersection set, the double-point set in the neighborhood of the triple point extends in six directions, like coordinate axes in three-space. If the axial arcs do not end in pinch points, they must meet up with another double-point arc emanating from the triple point, and the term for that is a *bridge*. If that bridge is the boundary of a disk in f(P), we call it an *untwisted bridge*. The case of untwisted bridges is completely covered in [CM]. However, in addition to the six immersions and generic surfaces of the projective plane presented in the Cromwell-Marar paper, there are a few additional ones that incorporate a twist similar to that in the immersion $\mathcal{G}$. One of the three additional surfaces is $\mathcal{G}$. In this section, we present the others and demonstrate that the list of immersions and generic surfaces of the projective plane with a single triple point and a connected self-intersection set is complete.

As we saw in the last section, the neighborhood of the self-intersection set is sufficient for determining if a specific configuration of bridges and pinch points is the projective plane in $\mathbb{R}^3$. The criteria from the last section encourage a specific focus on the edges of $N(\mathcal{S})$. To more easily illustrate the edges, we will "flatten out" the diagram to three overlapping circles, similar to ones found in Carter [C]. See Figure 4. The arcs in this diagram join up to create the boundary edges of $N(\mathcal{S})$.

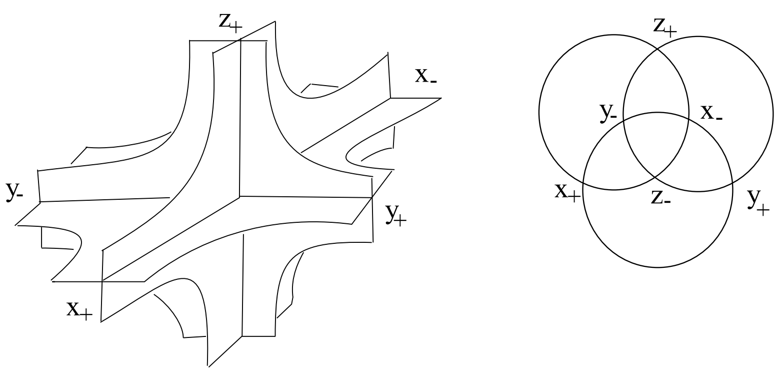

Figure 4

These diagrams can be adapted to show an untwisted or half-twisted bridge joining adjacent arcs as in figure 5a. As shown, we can either indicate the identifications to be made along the bridge, or make those identifications in the edge diagram (as on the right of 5a). In the case of the twisted bridge, we will generally eliminate the small kink in an edge for simplicity. It clearly does not affect linking. Pinch points can also be easily illustrated as shown in Figure 5b: an intersection simply turns into two non-intersecting arcs. Recall that a pinch-point can be directed in two ways, which leads to different surfaces.

Quarter-twisted bridges joining opposite arcs are significantly more difficult to illustrate, hence we simply indicate the identifications to be made. (Note that under this notation, a quarter-twist one way and a three-quarter twist the other way are identical.) Thus if we find a candidate with four edges, we will need to present the full $N(\mathcal{S})$, where we can more easily tell if the edges are linked.

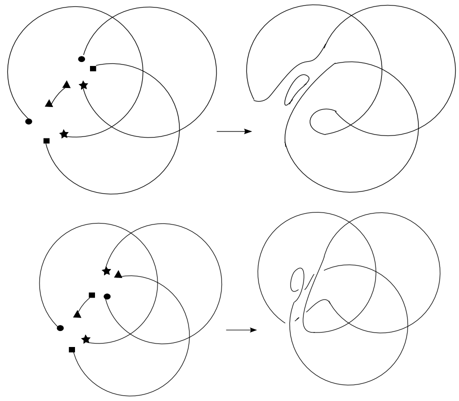

(a) adjacent bridges (untwisted and twisted)

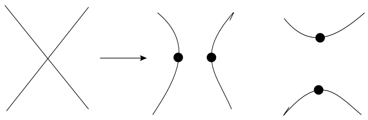

(b) pinch points

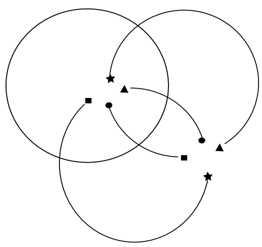

(c) quarter-twist bridge

Figure 5

The resulting diagram will be referred to as the *edge diagram*. Figure 6 shows the edge diagrams of $\mathcal{G}$ and the six Cromwell-Marar surfaces of the projective plane with a single triple-point and connected self-intersection set so that the reader can better understand how these diagrams work.

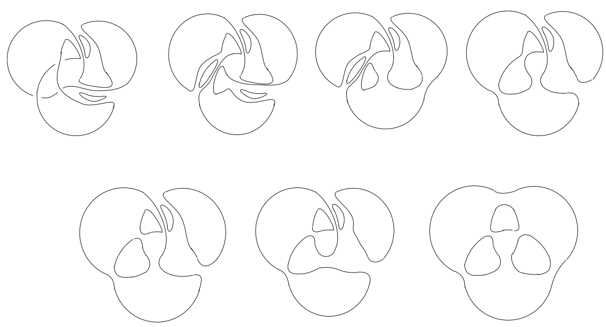

Figure 6. Girl's ($0'_A$), Boy's (0_A), 2_c, 4_A, 4_D, 4_F, Steiner's (6_A)

In this section, we aim to examine systematically all configurations of bridges to identify which represent the projective plane. The cases with six pinch points (hence no bridges) have been covered by Cromwell and Marar, and the cases with zero pinch points (immersions) have been covered by Goodman and Kossowski. Since pinch points come in pairs, we are left to examine configurations with four and two pinch points. We approach this task by considering the different configurations of bridges, and then considering in which directions we might add pinch-points. Oftentimes the bridges require certain directions in order to achieve at least four edges, one of the criteria from the last section.

Case I. One bridge and four pinch points.

Begin with configurations with one bridge and four pinch points. The case of an adjacent untwisted bridge is covered in Cromwell and Marar. So here, we consider the half-twisted adjacent bridge, and all configurations of the opposite bridge. By symmetry, the direction of the half-twist is irrelevant.

A. The adjacent twisted bridge case. Figure 7 is an edge diagram of an adjacent twisted bridge, before the direction of the pinch-points has been determined.

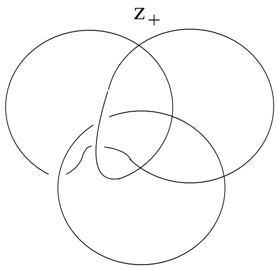

Figure 7

We claim that however we configure the pinch-points, fewer than four edges result. Each pinch point locally has two edges, one on each side. From the diagram we see that there are no edges without pinch points. With four edges and four pinch points, each with two local edges, on average each edge goes through two pinch points. Upon inspection of the diagram, there is no arc that connects a pinch point to itself, so each edge must go through at least two pinch points. Therefore, each edge must go through exactly two pinch points. With either direction for the pinch point at z_+, the edge going through z_+ also goes through two other pinch points, which is a contradiction. We hence conclude that there are fewer than four edges, and this configuration cannot lead to a projective plane.

B. The opposite bridge case. On the left of Figure 8a is the general edge diagram for an opposite bridge. In either twist direction, the argument is the same so we look at one case. Note that there is exactly one way to choose the direction of the pinch-points to create exactly four edges, illustrated on the right of Figure 8a. Because we did abandon the ability to check for linking, we are forced to examine $N(\mathcal{S})$. For a quarter-twist, the edges are unlinked as shown in Figure 8b, meaning this is a generic surface of the projective plane. To stay consistent with Cromwell and Marar, we will call this surface $4'_A$.

Notice that adding additional full twists, in either direction, along the bridge creates linking between any pair of edges along the bridge and hence could not completed in 3-space.

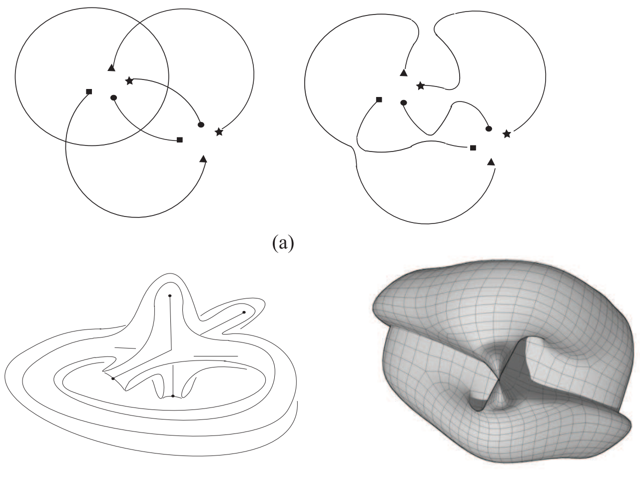

(a) (b) (c)

Figure 8

Case II. Two bridges and two pinch points

There are many more configurations in this scenario, but the arguments for whether they can have at least four edges are simpler.

By Corollary 1.4, the one pair of pinch points must be like oriented. The two pinch points are either opposite or adjacent to each other. If they are opposite, there can be two adjacent bridges or two opposite bridges. If they are adjacent there can be either two adjacent bridges, or an adjacent bridge and an opposite bridge.

A. Opposite pinch-points, with two opposite bridges. With the pinch points opposite each other, to be like oriented, pinch pair must have a Möbius band neighborhood (a non-well-aligned pairing in the language of [CM]). There are a few cases to consider: both bridges having quarter-twists in the same direction as shown in Figure 9a (twisting both in the other direction is symmetric), and one bridge with a quarter-twist in one direction and one in the opposite direction. This latter case has edge diagram is readily shown to have fewer than four edges. So we are left with one case to consider in detail.

Figure 9b is the space model corresponding to the edge diagram in 9a. The black shapes match up with other black shapes, as do the white shapes. The bridges have not been attached to preserve generality, though the double-point set for one of the bridges is presented. The goal is to show that either the boundary component with squares or the one with circles must be linked to the drawn double-point loop. Showing this will imply that completing the figure would require a disk-face intersecting the double-point set creating another triple-point and violating our hypothesis of a single triple point.

Let x be the linking number between the square boundary component and the double- point loop. Let y be the linking number between the circle boundary component and the double-point loop. If they are different, they cannot both be zero, and so one must be linked. The portion of the boundary component around the dark-shape bridge will change both x and y by the same number. However, the hollow-shape bridge will change the circle boundary component by an odd number and the square boundary component by an even number, as is observable by the fact that one hollow circle is inside the shape and one outside, whereas both hollow squares are outside. Therefore, x does not equal y.

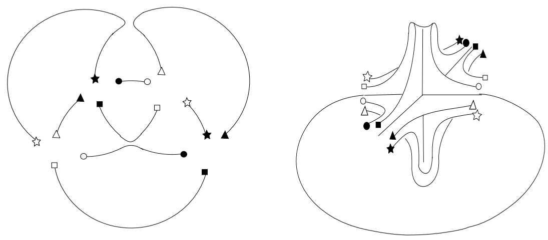

(a) (b)

Figure 9

B. Opposite pinch points and two adjacent bridges. *1. Two twisted bridges.* Of the twelve original arcs in the diagram in Figure 10a, four are joined to create one complete boundary edge passing by no pinch points. The bridges join the other arcs to create four longer arcs, each running from one pinch point to the other. Then the connections at each pinch point join pairs of these, hence there are fewer than four boundary edges to $N(\mathcal{S})$.

2. A twisted bridge and an untwisted bridge. The edge diagram is shown in Figure 10b. While only one direction of twist for the bridge is shown, it is easily seen that either direction produces linked edges and hence cannot be completed in 3-space.

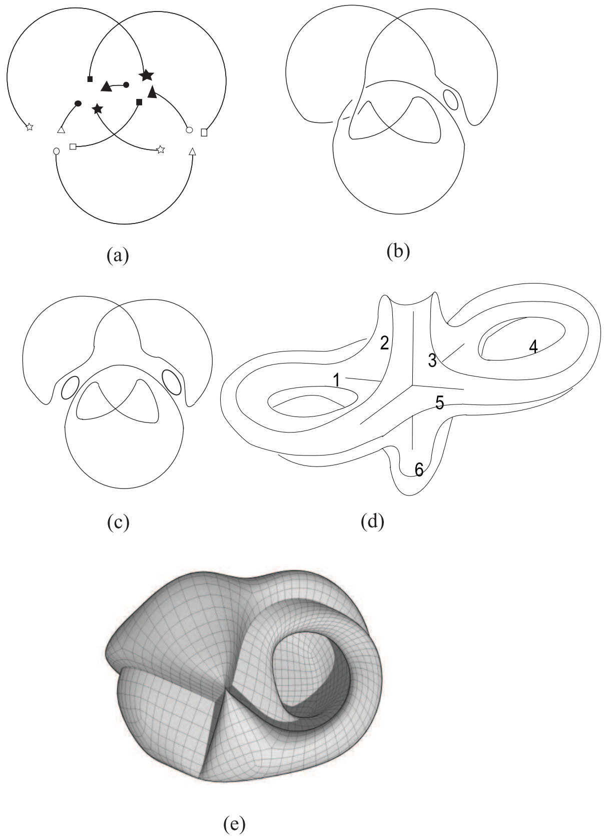

Figure 10

3. Two untwisted bridges. We again note that to be like oriented the pinch pair must have a Möbius band neighborhood; hence $N(\mathcal{S})$ is as shown in figure 10d. Note that there are six boundary edges so some faces must not be disks. By Proposition 1.6, $4 = f_1 - f_3 - 2f_4 - \cdots - (k-2)f_k$. In particular, the number of disk faces is at least four. Suppose some face has more than two boundary edges. Then there would be fewer than four remaining boundary components for disk faces, a contradiction. Therefore, if this configuration leads to the projective plane, it must be the case that two boundary edges match up to create an annular face, and the other four edges bound disks.

To see what these surfaces look like, notice that if every edge bounds a disk, the resulting cell complex would be the cross-cap intersected with the sphere. Therefore, to ensure our resulting complex is a single surface, the annular face must border a component from the sphere (1, 4 or 5) and a component from the cross-cap (2, 3 or 6). There are nine possible combinations, and after accounting for reflections leads to five: 1 and 2 (we call this surface $2''_D$), 1 and 3 (which cannot be completed since 1 and 3 are separated by the disks on 2, 4, and 6), 1 and 6 ($2''_B$), 5 and 2 ($2''_A$), 5 and 6 ($2''_C$).

The resulting four surfaces are similar. Each is the cross-cap surface with part of the face pushed through the double-point set to create a triple-point. Another way to think of it is as the sphere and cross-cap intersecting one another to create a triple point, and then attaching a handle somewhere between somewhere on the sphere and then somewhere on the cross-cap.

C. Adjacent pinch points. Now we consider the case where the pinch points are adjacent to one another. The configuration with two adjacent untwisted bridges has already been covered by Cromwell and Marar; the only projective plane model is 2A. Now consider the configurations with twisted bridges.

1. One opposite bridge, and one adjacent bridge, twisted or untwisted. The direction of twists is not important here; the same argument works regardless of direction. Edge diagrams for the twisted and untwisted adjacent bridge are shown in Figure 11a. The connections formed by the bridges create one complete edge and four arcs. Then at the z_+ pinch point, two pairs of these arcs are joined, leaving no possibility of four or more complete boundary edges.

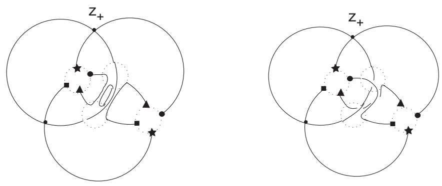

(a)

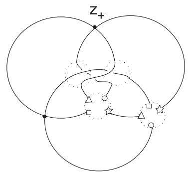

(b)

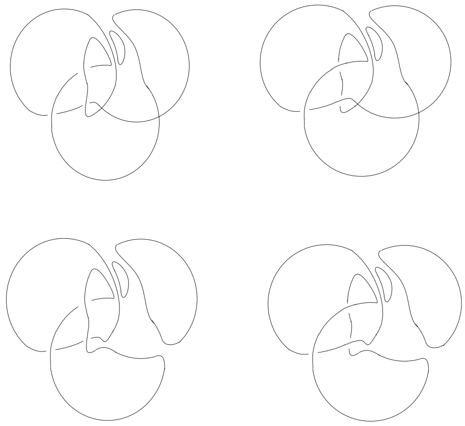

(c)

Figure 11

2. Two twisted adjacent bridges. The edge diagram for this configuration is shown in Figure 11b. After the connections for the bridges are made, there are four arcs (two running from the pinch point at z_+ to the one at y_- and one each from z_+ to itself, the last from y_- to itself. At least two distinct arcs are connected at z_+ so fewer than four boundary edges result.

3. Two adjacent bridges, one twisted and one untwisted. For each of the edge diagrams shown in Figure 11c, there is exactly one way to choose the direction of the pinch points to obtain four edges, illustrated in the second row of 11c. However, the one on the right has linked edges and cannot be completed in 3-space. However the one on the left gives another new generic surface: $2'_A$.

This completes the classification of generic maps of the projective plane with one triple point.

Section 3

In [GK] a classification of immersions of $\mathcal{P}$ with a single triple point was aided by analyzing the possible preimages of the self-intersection set (the "double-decker set" of [CS]) and tracking the changes in the preimage through Roseman-Homma-Nagase moves. In this section we will similarly trace deformations between the generic maps of the projective plane classified in the previous section.

Recall that two immersions $f, g : M \to \mathbb{R}^3$ are called *regularly homotopic* if there is a smooth mapping $H : M \times [0,1] \to \mathbb{R}^3$ such that H_t is an immersion for each t in [0, 1], and $H_0 = f$ and $H_1 = g$. One can extend this notion to generic maps by requiring that each H_t be an immersion except at pinch points. (See [J] for further details.) Pinkall [P] classified immersions of surfaces into $\mathbb{R}^3$ up to regular homotopy, allowing diffeomorphisms of the surface. Juhász [J] proved that any two generic maps with singularities of the same surface are regularly homotopic if and only if they have the same (positive) number of pinch points. In this section, it is our aim is to illustrate these results as they apply to the specific surfaces we have been considering by tracking changes in the preimage.

For the projective plane, there are precisely two regular homotopy classes of immersions [H], [JT]. We will demonstrate that $\mathcal{B}$ and $\mathcal{G}$, with similarly-oriented self-intersection sets, represent these two equivalence classes. Following that, using just a couple of Roseman moves, we constructively show that all the generic maps with two pinch points are regularly homotopic, as are all the maps with four pinch points. Finally, using one additional Roseman move that pinches off a loop on the surface to create a pair of pinch points (hence no longer staying within a regular homotopy class), we illustrate how to move between all the surfaces of the last section.

Pinkall [P] defines a $\mathbb{Z}_4$-valued quadratic form that is an invariant on immersed surfaces . For the two regular homotopy classes of the projective plane, Pinkall shows this invariant reduces to the direction of the twist of a Möbius band somewhere on the immersed surface. There is a right-handed Möbius band on $f(\mathcal{P})$, if and only if $f(\mathcal{P})$ is homotopic to (the right-handed) Boy's surface.

Hence the problem has been reduced to finding a Möbius band somewhere on both $\mathcal{B}$ and $\mathcal{G}$ and seeing if they twist in the same direction or in opposite directions. For either, the immersed loop which is the self-intersection set is an orientation-reversing loop.

Let $f : \mathcal{P} \to \mathbb{R}^3$ be an immersion yielding $\mathcal{B}$ and $g : \mathcal{P} \to \mathbb{R}^3$ giving $\mathcal{G}$. Let $\alpha_{\mathcal{B}}$ (respectively $\alpha_{\mathcal{G}}$) be a loop going directly through the self-intersection set on the pre-image, with corresponding ε-neighborhood $\Psi_{\mathcal{B}}$ ($\Psi_{\mathcal{G}}$). The neighborhoods $\Psi_{\mathcal{B}}$ and $\Psi_{\mathcal{G}}$ map to Möbius strips since their core is an orientation-reversing loop in the pre-image. Now consider the difference between $f(\Psi_{\mathcal{B}})$ and $g(\Psi_{\mathcal{G}})$. $g(\Psi_{\mathcal{G}})$ is almost identical to $f(\Psi_{\mathcal{B}})$ but has two half-twists as it goes around the twisted loop twice. This adds a full twist, meaning if $g(\Psi_{\mathcal{G}})$ is a right-twisted Möbius strip, then $f(\Psi_{\mathcal{B}})$ is a left-twisted Möbius strip, and vice versa.

This is best illustrated by the set $N(\mathcal{S})$ for each of the immersed surfaces. If one carefully follows a strip, going through the triple-point six times over, almost the exact same path is followed for $\mathcal{B}$ or $\mathcal{G}$, with the only difference being a half-twist each time one traverses around the twisted bridge. We can conclude $\mathcal{B}$ and $\mathcal{G}$ are homotopically distinct.

In the next discussion we will not consider the surfaces with annular faces since, as noted in section 2, they can be viewed as the cross-cap with part of the surface pulled through the self-intersection set to create a triple point. It is then trivial to note that all four are regularly homotopic to the cross-cap, and by extension 2_A and $2'_A$.

One of the key tools we use for demonstrating a deformation between the other surfaces is the plane model of $\mathcal{P}$. To get a plane model representation of any of the generic maps, we use a procedure developed in [GK]. The preimage in $\mathcal{P}$ of a neighborhood of the triple point T consists of three components, each homeomorphic to a neighborhood of one of the three preimages of T, as shown in Figure 12a. Information about how the ends of these components are identified allows us to reconstruct the self-intersection set as a graph in $\mathcal{P}$. For a bridge, connect the ends of the double-point arcs of the corresponding slices (with twists as needed). For pinch-points, connect ends of the double point set corresponding to the same axial arc (e.g. the positive x-axis to itself), again respecting the orientation of the pinch point. The dot on the graph indicates a pinch point. One example ($2'_A$) is illustrated in Figure 12b.

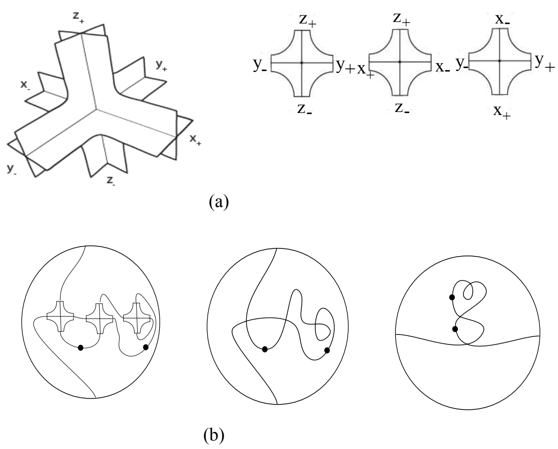

Figure 12

Preimage graphs for the other generic surfaces from Section 2 are shown in Figure 13.

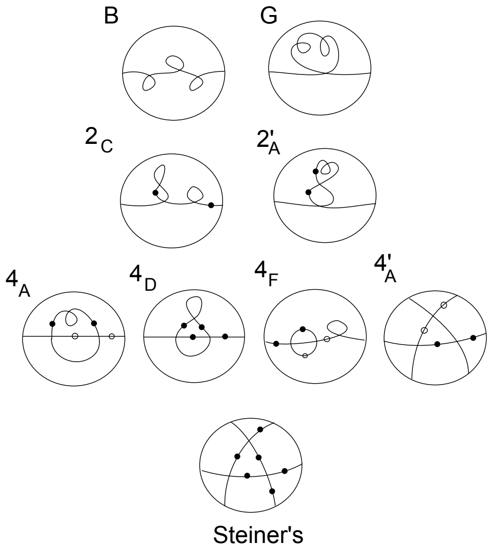

Figure 13

While the plane models make it easy to demonstrate the Roseman moves transforming one surface to one another, there are limitations: the direction of a twist is not apparent and one cannot determine if the surface is realizable in space.

We use the two Roseman moves in Figure 14 (a) and (b) to illustrate the regular homotopies between generic surfaces with the same number of pinch points. The left figures illustrate the moves in space and the right in the local changes in the plane model.

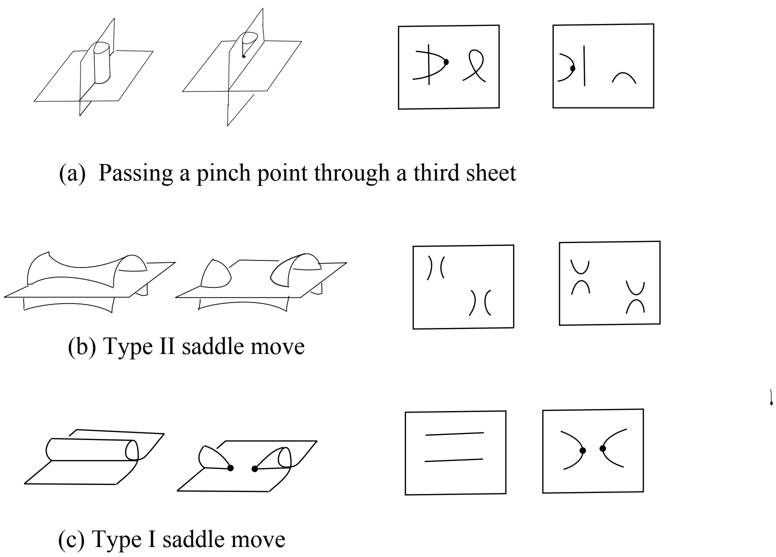

(a) Passing a pinch point through a third sheet

(b) Type II saddle move

(c) Type I saddle move

Figure 14

We use one other Roseman move (Figure 14c) to transform to a generic surface with a different number of pinch points (which changes the regular homotopy class of the surface).

If (x) is a move from the above list, we will use (x^{-1}) to denote doing the inverse move. Note the moves (a) and (a^{-1}) are local, meaning that if the move can be done in the plane model, then it can be done in space. However, the others require certain configurations of the surface in space. The (c^{-1}) move requires that the pinch-points be like-oriented, while (c) requires that the loop being pinched off bounds a disk in space not meeting the surface. The (b)-move requires that two paths (A and B in figure 15) with ends at points of the self-intersection set and lying on different sheets of the surface bound a disk not meeting the surface.

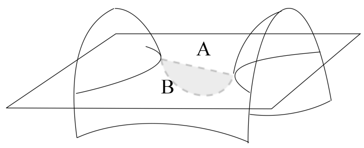

Figure 15

A single application of the (a) move transform the generic surfaces 2_A and $2'_A$ to the cross-cap surface. So to get from one to the other, one only need apply (a) and then (a^{-1}). Note that since (a) and (a^{-1}) are local moves, showing the change in the plane model is sufficient. Similarly 4_A, 4_D and 4_F can be homotoped to the cross-cap with a pinch-point blister after a single (a) move.

This leaves $4'_A$. Note that one cannot apply move (a) to it. Rather one must use a (b) move to get to 4_A, and we must verify in the space model that one can perform the appropriate move.

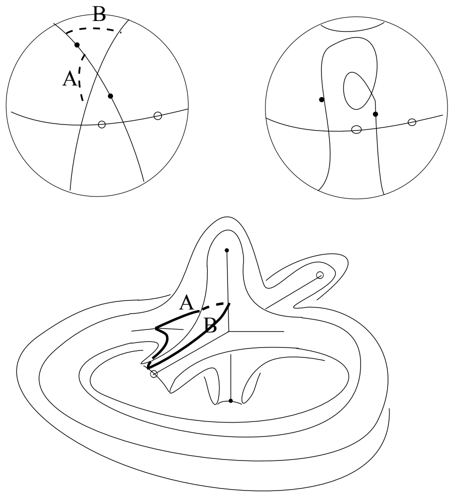

Figure 16

Finally, to illustrate transformations taking a generic surface with $2k$ pinch points to one with $2k-2$ pinch points (hence changing the regular homotopy class) we use the (c^{-1}) move. We need only check that the pinch points that are to be merged are like oriented. We add some notation to the plane diagrams to indicate like-oriented pinch points. Having chosen a side of the image surface to be the positive side, one can readily identify single-sheeted and double-sheeted pinch points. That information is encoded into the plane diagram as follows. Pinch points will be indicated by open or filled circles (shown on the chart in Figure 13). Those of the same type are like-oriented to each other and can be merged.

Begin with Steiner's surface 6_A. All the pinch points are similarly oriented so we can merge any pair where we have a clear merge path. The symmetry of Steiner's surface makes it easy to check that whichever two pinch points one chooses to apply (c^{-1}) to, the resulting generic surface is 4_D. (This is also clearly the only possibility since it is the only generic surface with all four pinch points similarly oriented.)

Note that when one applies (c^{-1}) on 4_A , one pair has no clear merge path. Merging the other pair (along either possible merge path) disconnects the preimage graph, producing an annular face. It is possible to merge to either $2''_A$ or $2''_B$.

There are several ways of merging pairs of pinch points on 4_D, three of which lead to 2_C , two to $2'_A$, and one to each of $2''_C$ and $2''_D$. For 4_F, any choice of like-oriented pinch points yields either 2_D or $2'_A$ depending on the choice of merge path.

The $4'_A$ surface allows no possible path to merge pinch points. Of course, if one first performed a regular homotopy to another of the 4-pinch surfaces, one could then merge to 2_D or $2'_A$.

Merging the two pinch points of 2_A takes the surface to either $\mathcal{B}$ or $\mathcal{G}$, depending on the choice of merge path. Interestingly, merging the pinch points on transform the surface to $\mathcal{G}$, but $\mathcal{B}$ is not possible since there is a twisted bridge.

The above transformations are summarized in Figure 17.

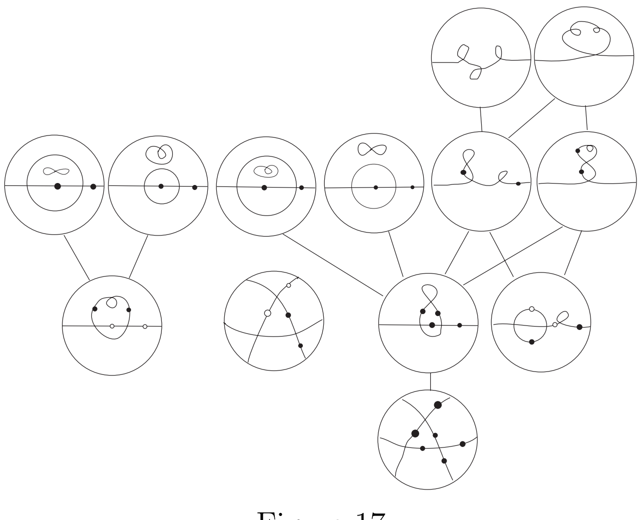

Figure 17

References

[A] Apery, F. *Models of the Real Projective Plane.* Braunschweig: Vieweg, 1987.

[B] Banchoff, Thomas F. "Triple Points and Surgery of Immersed Surfaces." *Proceedings of the American Mathematical Society*, 1974: 407–413.

[C] Carter, J.S. *How Surfaces Intersect in Space*, World Scientific, 1993.

[CS] Carter, J.C. and M. Saito, *Knotted Surfaces and Their Diagrams*, Mathematical Surveys and Monographs, vol. 55, AMS, 1998.

[CM] Cromwell, Peter R., and W.L. Marar. "Semiregular Surfaces with a Single Triple Point." *Geometriae Dedicata*, 1994: 143–153.

[FT] Fenn, R. and P. Taylor, On the number of triple points of an immersed surface, (unpublished) preprint (1977).

[GK] Goodman, Sue and Mark Kossowski. "Immersions of the Projective Plane with one triple point." *Differential Geometry and its Applications* **27**, 2009.

[HH] Hass, Joel and John Hughes. "Immersions of Surfaces in 3-Manifolds." *Topology* **24**, 1985: 97–112.

[H] Hirsch, M.W. "Immersions of Manifolds." *Trans. of the American Mathematical Society*, 1959: 242–272.

[IM] Izumiya, S. and W.L. Marar. "The Euler Characteristic of a Generic Wavefront in a 3- Manifold." *Proceedings of the American Mathematical Society*, 1993: 1347–1350.

[JT] James, Ioan and Emery Thomas. "Note on the Classification of Cross-Sections." *Topology* **4**, 1966: 351–359.

[J] Juhász, András. "Regular homotopy classes of local generic mappings." *Topology and its Applications* **138**, 2004: 45–59.

[NS] Nuño Ballesteros, J.J. and Saeki, O. "Euler characteristic formulas for simplicial maps." *Math. Proc. Camb. Phil. Soc.*, 2001: 307–331.

[P] Pinkall, U. "Regular Homotopy Classes of Immersed Surfaces." *Topology* **24**, 1985: 421–434.

[S] Samelson, Hans. "Orientability of Hypersurfaces in R^n." *Proc. of American Mathematical Society*, 1969: 301–302.

[W] Whitney, Hassler. "The Singularities of a Smooth n-Manifold in $(2n-1)$ Space." *Annals of Mathematics*, 1944: 247–293.